From a mononuclear $Fe^{II}L_2$ complex to a spin crossover $Fe^{II}_4L_6$ cage by symmetric ligand architecture modification: insights into the ammonia gas sensing mechanism

Weiyang Li,[a] Aurelian Rotaru,[b] Mariusz Wolff,[c] Serhiy Demeshko,[d] Franc Meyer,[d] Yann Garcia[*a]

[a] Institute of Condensed Matter and Nanosciences, Molecules, Solids, Reactivity (IMCN/MOST), Université catholique de Louvain, Place Louis Pasteur 1, 1348 Louvain-la-Neuve, Belgium

[b] Department of Electrical Engineering and Computer Science and MANSiD Research Center, "Stefan cel Mare" University, University Street, 13, Suceava 720229, Romania

[c] Institut für Chemische Katalyse, Universität Wien, Währinger Strasse 38, 1090 Wien, Austria

[d] Institut für Anorganische Chemie, Universität Göttingen, Tammannstrasse 4, D-37077 Göttingen, Germany

Contents

General information

All the chemicals and solvents were commercially available and were used without further purification. ^1H NMR and ^{13}C NMR spectra were recorded on a Bruker AVANCE 300MHz spectrometer. Electrospray ionization time-of-flight mass spectrometry (ESI-TOF-MS) were collected on a Bruker maXis UHR ESI-Qq-TOF mass spectrometer in the positive ion mode. Elemental analysis (C, H, and N) was measured by MEDAC Ltd, UK. Powder X-ray diffraction (XRD) measurements were carried out at room temperature on a Bruker D8 ADVANCE X-ray diffractometer with Cu Kα radiation ($\lambda = 1.5148$ Å). Fourier transformed infrared (FT-IR) spectra were performed on Equinox 55 (Bruker) equipped with an ATR modulus and an MCT detector. The micromorphology was studied by field emission scanning electron microscopy (SEM) using a Mira3-TESCAN microscope from Oxford Instruments Inc. Thermogravimetric analyses (TGAs) were carried out by Mettler Toledo TGA/SDTA 851e analyzer in $N_{2(g)}$ (100 mL min^{-1}) at a heating rate of 10 ^{o}C min^{-1} between 25 ^{o}C and 850 ^{o}C. The specific surface area was obtained by analyzing the nitrogen absorption and desorption curves measured on Micromeritics ASAP 2020. Diffuse reflectance spectra (DRS) were performed with a PerkinElmer Lambda 9 UV/vis/NIR spectrophotometer and converted into absorption spectra by using the Kubelka−Munk function, using $BaSO_4$ as a reference. Magnetic susceptibility was measured on a Quantum design MPMS-5S (for **1**) or MPMS3 (for **2**) SQUID magnetometers and the magnetic data were corrected for the sample holder and diamagnetic contributions. ^{57}Fe Mössbauer spectra for **1**, **1**@NH$_3$, regenerated **1**, **2**@NH$_3$ and regenerated **2** were recorded at 298 K using a constant acceleration Wissel Mössbauer spectrometer operated in the transmission mode and equipped with a Reuter Stokes proportional counter. ^{57}Fe Mössbauer spectra for **2** at low temperatures (7 K and 80 K) were recorded using an alternating constant acceleration Wissel Mössbauer spectrometer operated in the transmission mode and equipped with a Janis closed-cycle helium cryostat. The Mössbauer spectrum of **2** at 295 K was recorded using an alternating constant acceleration Wissel Mössbauer spectrometer operated in the transmission mode and equipped with an OptiCool closed-cycle helium cryostat from Quantum Design. All spectra were fitted by the Recoil 1.05 Mössbauer Analysis software, except **2** (fitted with the Mfit program (E. Bill, Max-Planck Institute for Chemical Energy Conversion, Mülheim/Ruhr, Germany)). A home-made device was used for the sensing experiments (Fig. S4). The experiments were performed in triplicate at room temperature (25±1 °C).

Experimental Section

Synthesis of *N*-amino-1,8-naphthalimide
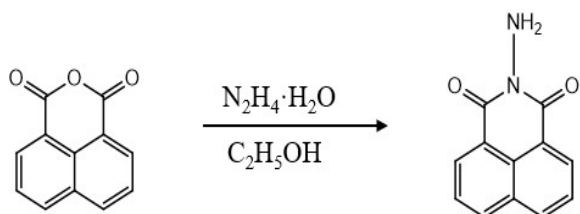
Scheme: synthesis method of *N*-amino-1,8-naphthalimide.

N-amino-1,8-naphthalimide was synthesized via a condensation reaction between 1,8-naphthalic anhydride (10 mmol, 1.98 g) and hydrazine hydrate (10 mmol, 0.5 g) in 50 ml methanol. A light-yellow colour solid was separated out after 8 h. The precipitate was filtered out and recrystallized in methanol. Yield: 1.8 g, 85%. ^{1}H NMR (DMSO-d_6, 300 MHz, ppm) δ: 8.47 (m, 4H), 7.86 (t, 2H), 5.78 (s, 2H); ^{13}C NMR (75 MHz, DMSO-d_6) δ: 160.58, 134.64, 131.33, 127.33, 126.05, 121.78. ESI-MS (*m/z*): calcd. for $C_{12}H_8N_2O_2$, 213.0658; found, 213.0658. Melting point: > 260 °C.
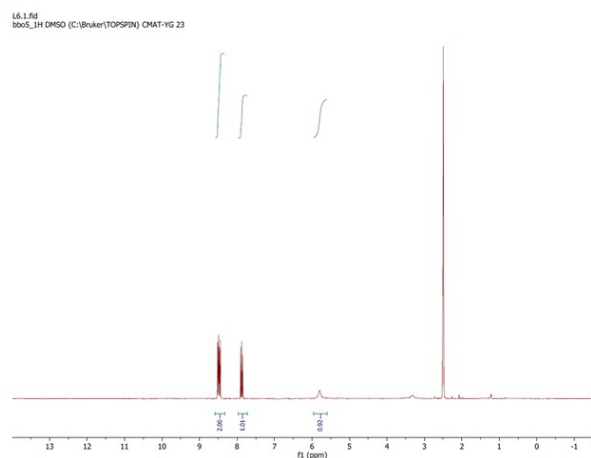
^{1}H NMR spectrum for *N*-amino-1,8-naphthalimide.
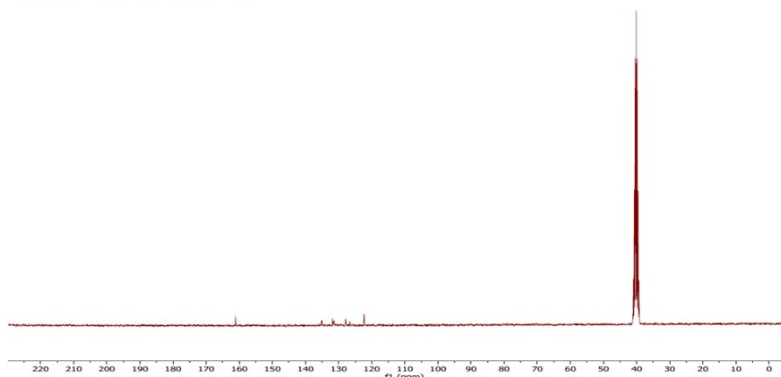
^{13}C NMR spectrum for *N*-amino-1,8-naphthalimide.

Synthesis of **1**
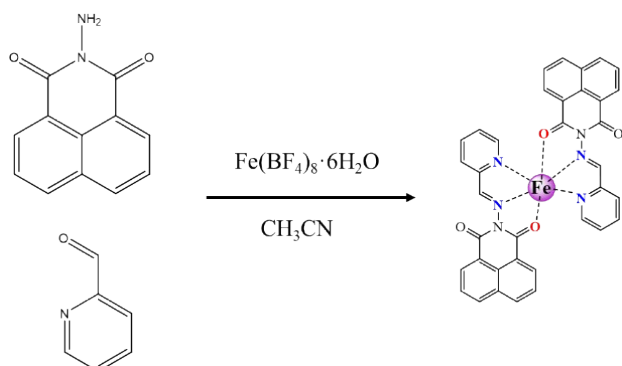
Scheme: Synthesis method of **1**.

N-amino-1,8-naphthalimide (42.4 mg, 0.2 mmol), 2-formylpyridine (19.1 μL, 0.2 mmol) and Fe(BF$_4$)$_2$·6H$_2$O (33.7 mg, 0.1 mmol) were added to Schlenk flask with acetonitrile (30 mL). The reaction mixture was stirred under Ar$_{(g)}$ at 50 °C overnight and then cooled to room temperature. The resulting purple solution was filtered and vapor-diffused with diethyl ether. After two weeks, purple crystals suitable for single-crystal X-ray diffraction analyses were obtained. Yield: 10.8 mg, 33% (based on the Fe(II) salt). Elemental analysis calcd. for [C$_{36}$H$_{22}$O$_4$N$_6$Fe](BF$_4$)$_2$, C 51.97%, H 2.66%, N 10.1%; found: C 52.16%, H 2.95%, N 10.09%. ESI-MS (*m/z*): calcd. for [C$_{36}$H$_{22}$O$_4$N$_6$Fe](BF$_4$)$_2$, 328.0543; found, 328.0541.

Synthesis of amorphous **2**
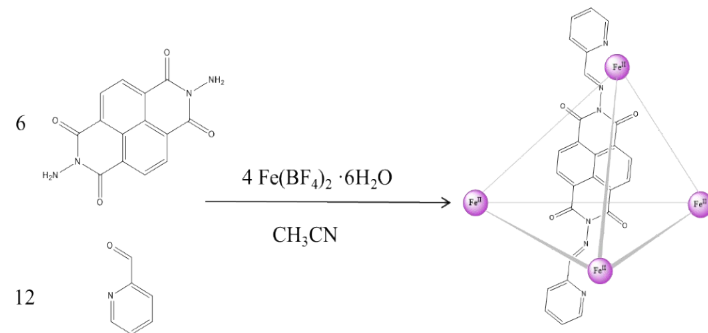
Scheme: Formation of **2** through subcomponent self-assembly.

The synthesis of subcomponent ligand N, N-diaminonaphthalene-1,4,5,8-tetracarboxydi-imide was prepared according to the literature procedure.[1] $Fe(BF_4)_2 \cdot 6H_2O$ (28.1 mg, 0.083 mmol), 2-formylpyridine (23.8 µL, 0.25 mmol) and N,N-diaminonaphthalene-1,4,5,8-tetracarboxydi-imide (37 mg, 0.125 mmol) were added to Schlenk flask with acetonitrile (40 mL). The mixture was stirred under argon at 65 °C overnight and then cooled to room temperature. The purple solution obtained was filtered and a large amount of diethyl ether was added to it. The light purple precipitate was filtered and washed five times with an excess of diethyl ether and dried. Yield: 61.6 mg (76%). Elemental analysis calcd. for $[C_{156}H_{84}N_{36}O_{24}Fe_4](BF_4)_8 \cdot 10H_2O$, C 47.50%, H 2.66%, N 12.78%; found C, 47.37%; H, 2.70%; N, 12.58%. ESI-TOF-MS: the following picked signals are those at the high intensities. m/z Calcd. for $[Fe_4L_6(BF_4)_5]^{3+}$ 1167.8024, found 1167.8020; Calcd. for $[Fe_4L_6(BF_4)_4]^{4+}$ 854.3508, found 854.3507; Calcd. for $[Fe_4L_6(BF_4)_3]^{5+}$ 666.0798, found 666.0799; Calcd. for $[Fe_4L_6(BF_4)_2]^{6+}$ 540.5658, found 540.5660; Calcd. for $[Fe_4L_6(BF_4)]^{7+}$ 450.9129, found 450.9130; Calcd. for $[Fe_4L_6]^{8+}$ 383.6732, found 383.6734.

Single-crystal X-ray diffraction analyses

X-ray diffraction analyses for complex **1** at 120 K and 298 K was carried on MAR345 image plate using Mo-Kα radiation (λ = 0.71073Å), generated by an Incoatec IµS generator equipped with Montel Mirrors. Data integration and reduction were performed with CrysAlis[PRO] (CrysAlis[PRO] Software System, Vol. Rigaku Corporation: Oxford, UK, 2015.) and the implemented absorption correction was applied. The structures were solved by SHELXT and refined by full-matrix least squares on F^2 using SHELXL2018/3. The location of the Fe atom was easily determined, and O, N and C atoms were subsequently located in the Fourier difference maps. Final crystallographic data and refinement values for **1** at 120 K and 298 K are listed in Tables S1. CCDC 2241853 and 2241857 contains the supplementary crystallographic data for this paper.

SHELXT:

Sheldrick, G. M. (2015). *Acta Cryst.* A**71**, 3-8.

Crysalis[PRO]:

Rigaku (2015). *CrysAlisPro Software System*, Version 1.171.38.41. Rigaku Oxford Diffraction

Table **S1.** Crystal data and structure refinement details for **1** at 120 K and 298 K.

Temperature	120 K	298 K
Formula	$C_{36}H_{22}FeN_6O_4 \cdot (BF_4)_2$	$C_{36}H_{22}FeN_6O_4 \cdot (BF_4)_2$
Formula weight	832.06	832.06
Radiation (Å)	MoK_α (0.71073)	MoK_α (0.71073)
Crystal system	Monoclinic	monoclinic
Space group	$P2_1/c$	$P2_1/c$
a (Å)	8.34709(14)	8.6034(2)
b (Å)	15.0978(4)	15.1618(4)
c (Å)	27.3487(5)	27.2871(6)
α (°)	90	90
β (°)	90.9970(15)	91.621(2)
γ (°)	90	90
V (Å^3)	3446.04(12)	3558.01(15)
Z	4	4
ρ_{calc} (g.cm^{-3})	1.604	1.553
Absorption coefficient (mm^{-1})	0.533	0.516
θ range (deg)	2.8450 to 26.2100	2.8350 to 26.0770
F(000)	1680	1680
Crystal size (mm)	0.3×0.1×0.07	0.3×0.1×0.07
Reflections collected	24108	24904
Independent reflections	6823 [$R_{(int)}$ = 0.0270]	7063 [$R_{(int)}$ = 0.0306]
Data/restraints/parameters	6823/50/546	7063/60/546
Goodness of fit on F^2	1.042	1.028
$R_1{}^a, wR_2{}^b$ (I>2σ(I))	0.0521, 0.1338	0.0719, 0.1763
$R_1{}^a, wR_2{}^b$ (all data)	0.0574, 0.1378	0.0880, 0.1860

Table **S2.** Fe−N bond lengths (Å) for complex **1** at 120 K and 298 K.

	120 K	298 K
Fe(1)-N(2)	2.177 (2)	2.159 (3)
Fe(1)-N(9)	2.169 (2)	2.166 (3)
Fe(1)-N(32)	2.149 (2)	2.156 (3)
Fe(1)-N(39)	2.193 (2)	2.181 (3)
Fe(1)-O(12)	2.143 (2)	2.142 (3)
Fe(1)-O(42)	2.087 (2)	2.089 (3)
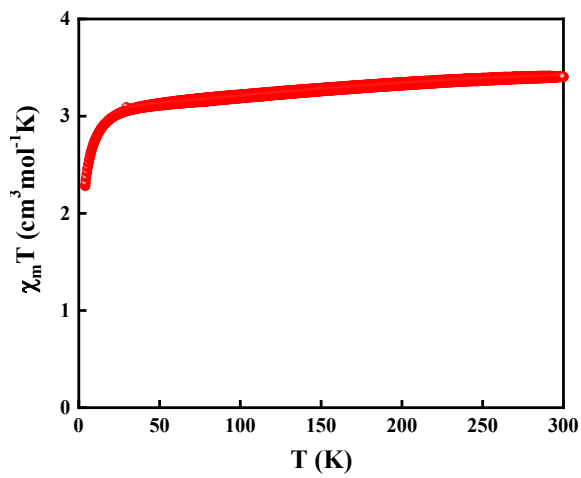
Fig. S1 Temperature-dependent $\chi_m T$ vs T plots for **1**.

C=N groups

BF$_4^-$

Fig. S2 FT-IR for **1**.

(a)

(b)
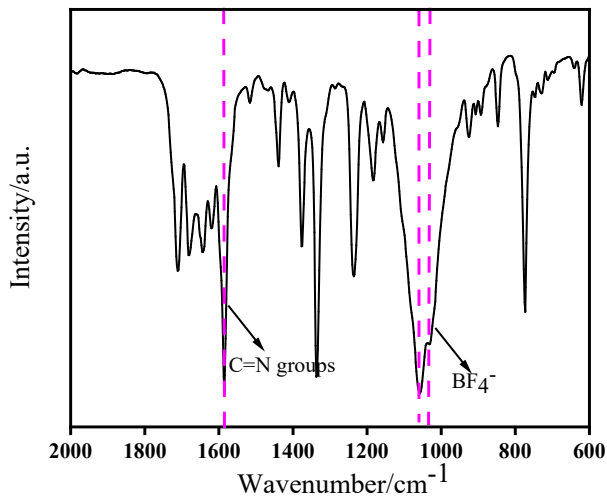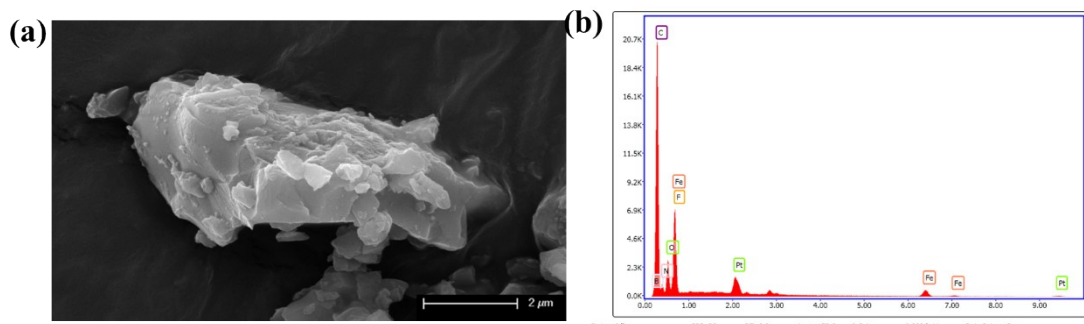
Fig. S3 SEM image (a) and EDS spectrum (b) for **1**. Pt signals are from sample preparation.
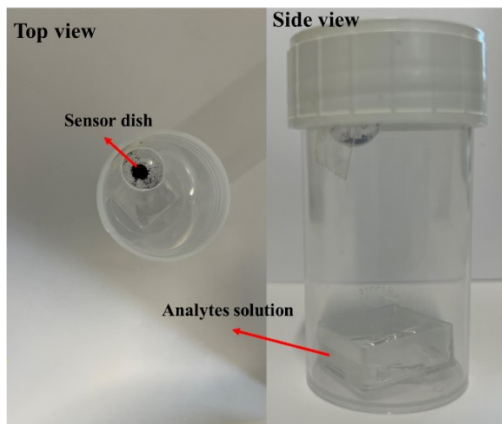
Fig. S4 Top and side view of the home-made sensor device. The diameter of the bottle is 3.5 cm and the volume is 50 mL. In each experiment, approximately 5 mg of the sensor sample and 0.5 mL of different analyte solutions were added to two separate trays. Colour-changing photos are recorded at specific times by iPhone 13, set to "Photo Mode" "Tap to Focus" and "No Flash".
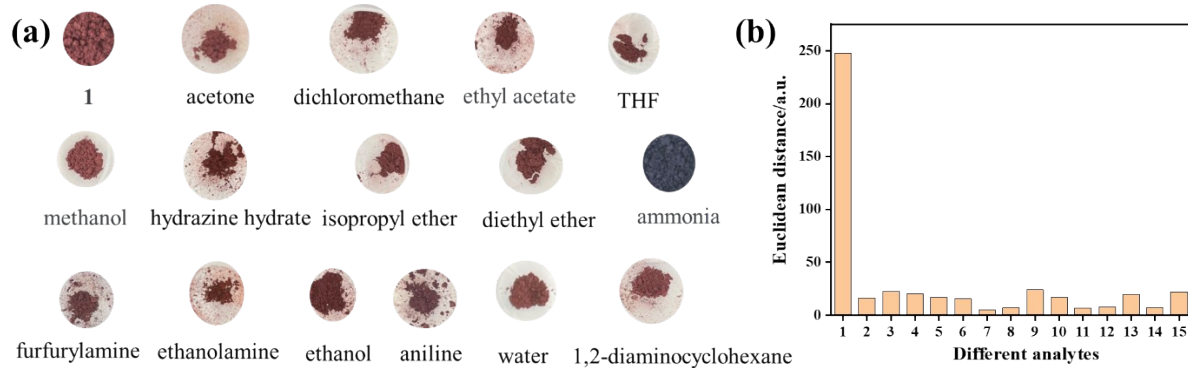
Fig. S5 (a) Digital photographs and (b) corresponding Euclidean distances and of **1** after exposure to 15 analytes at full vapor pressure at room temperature. $1 = NH_3$; $2 =$ ethanol; $3 =$ hydrazine hydrate; $4 =$ methanol; $5 = 1,2$-diaminocyclohexane; $6 =$ diethyl ether; $7 =$ isopropyl ether; $8 =$ tetrahydrofuran; $9 =$ ethanolamine; $10 =$ ethyl acetate; $11 =$ dichloromethane; $12 =$ acetone; $13 =$ furfurylamine; $14 =$ water; $15 =$ aniline.
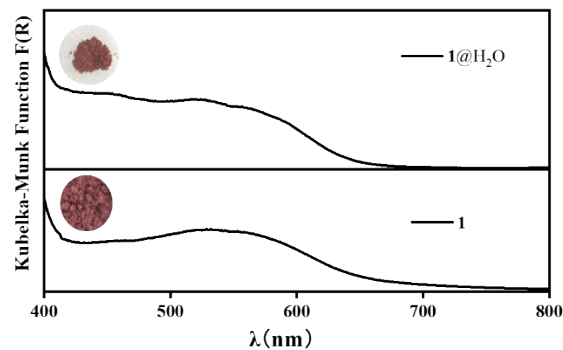
Fig. S6 Diffuse reflectance spectrum of **1** and **1**@H_2O.
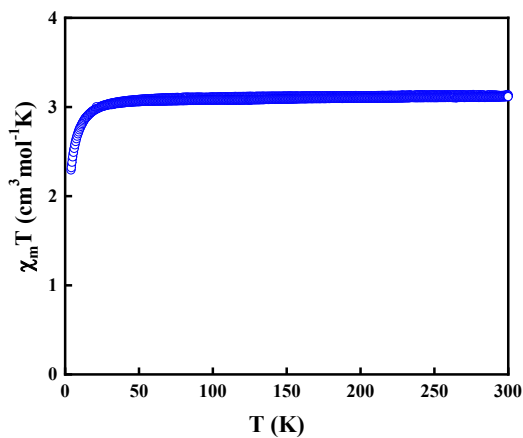
Fig. S7 Temperature-dependent $\chi_m T$ vs T plots for **1**@NH$_3$.
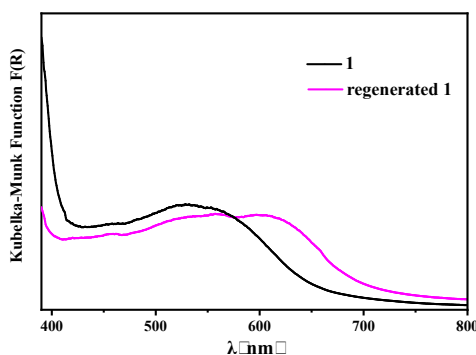
Fig. S8 Diffuse reflectance spectrum of regenerated **1**.
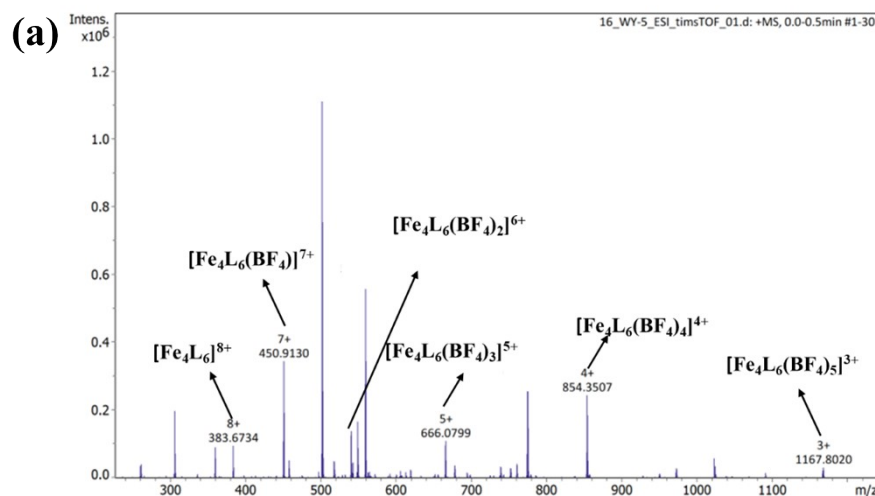
Fig. S9a ESI-TOF-MS spectrum of **2**.
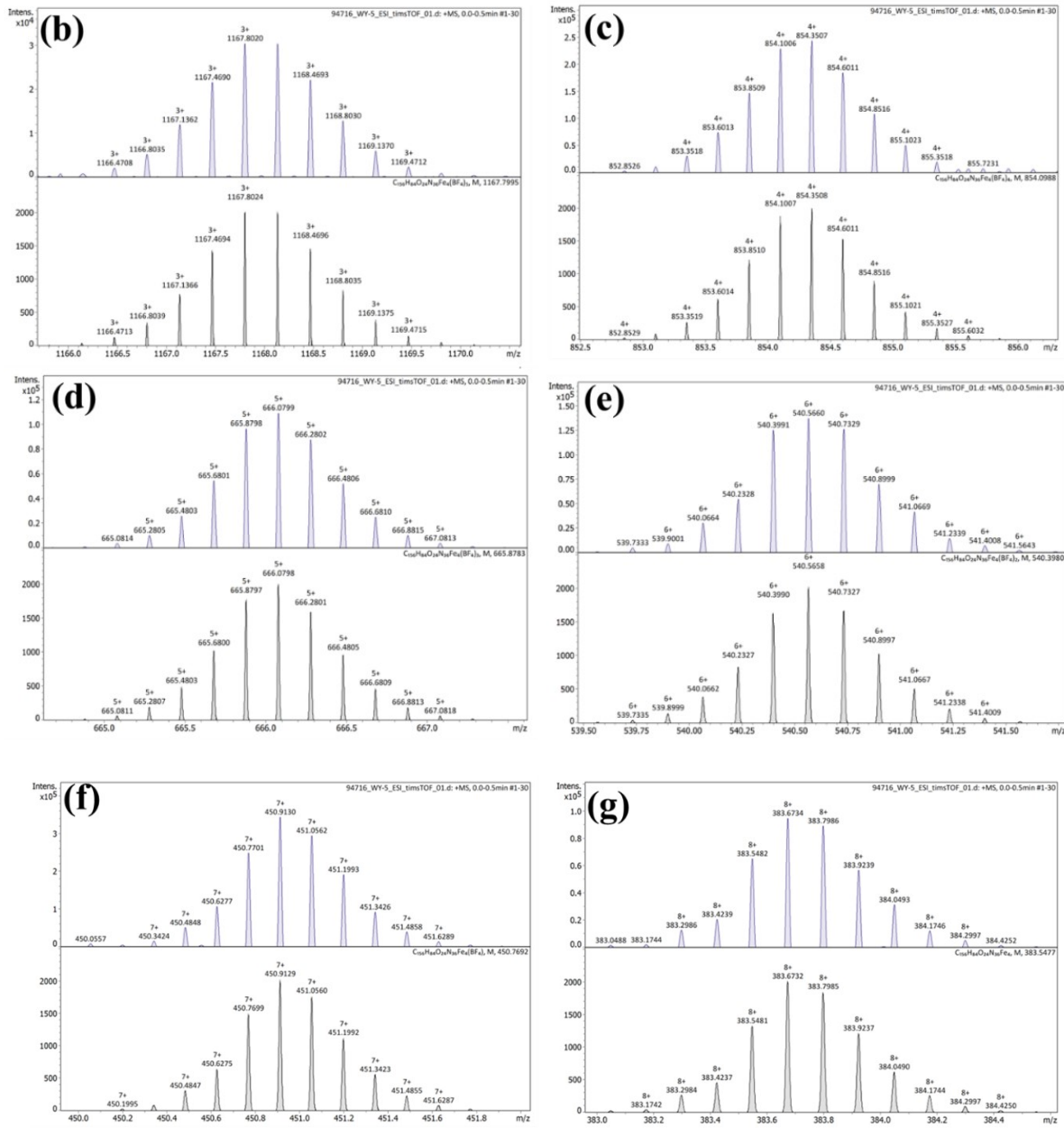
Fig. S9b-S9g Comparison of the observed isotopic patterns with the simulated spectra for different charge states from 3+ to 8+ of **2**.
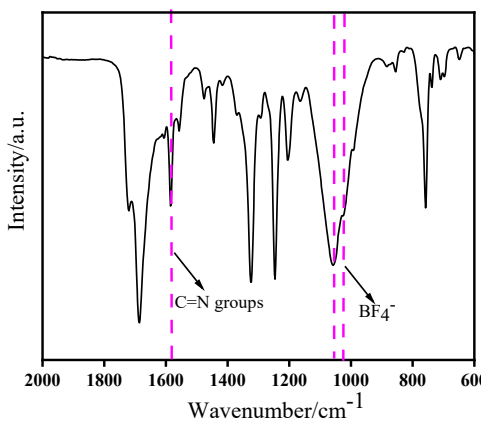
Fig. S10 FT-IR for **2**.
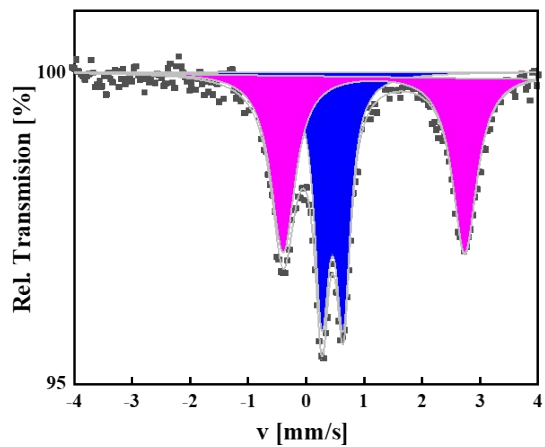
Fig. S11 ^{57}Fe Mössbauer spectrum of **2** recorded at 7 K.
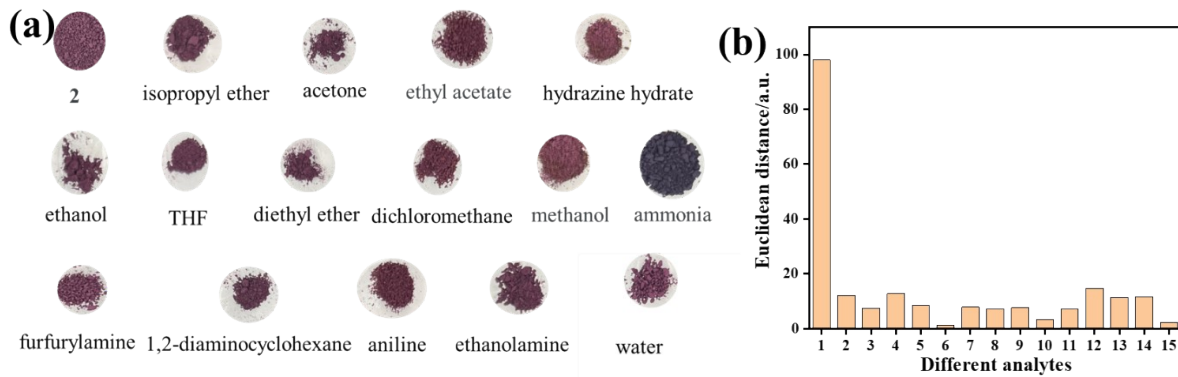
Fig. S12 (a) Digital photographs and (b) corresponding Euclidean distances and of **2** after exposure to 15 analytes at full vapor pressure at room temperature. $1 = NH_3$; $2 =$ hydrazine hydrate; $3 =$ methanol; $4 =$ furfurylamine; $5 =$ ethanol; $6 =$ diethyl ether; $7 =$ acetone; $8 =$ isopropyl ether; $9 =$ tetrahydrofuran; $10 =$ dichloromethane; $11 =$ ethyl acetate; $12 = 1,2$-diaminocyclohexane; $13 =$ aniline; $14 =$ ethanolamine; $15 =$ water.
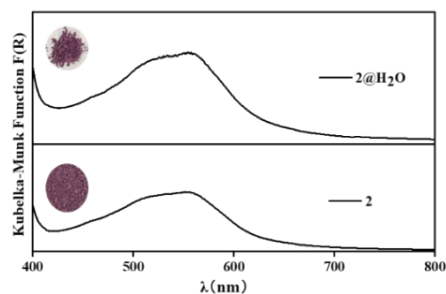
Fig. S13 Diffuse reflectance spectrum and digital images of **2** and **2**@H_2O.
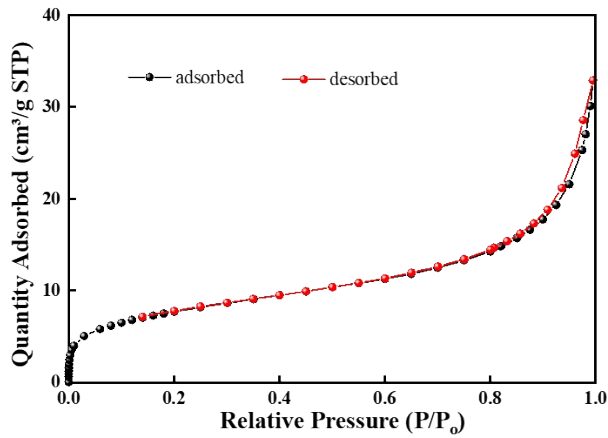
Fig. S14 Nitrogen adsorption-desorption isotherms of **2**.
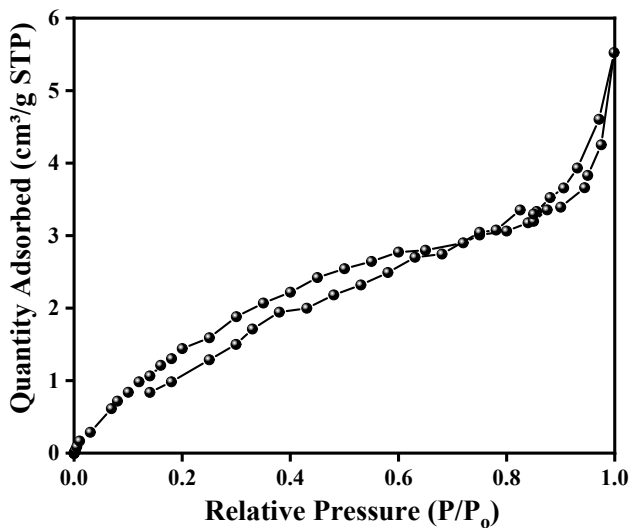
Fig. S15 Nitrogen adsorption-desorption isotherms of **1**.

All BF$_4^-$ anions are on the outside of the cage
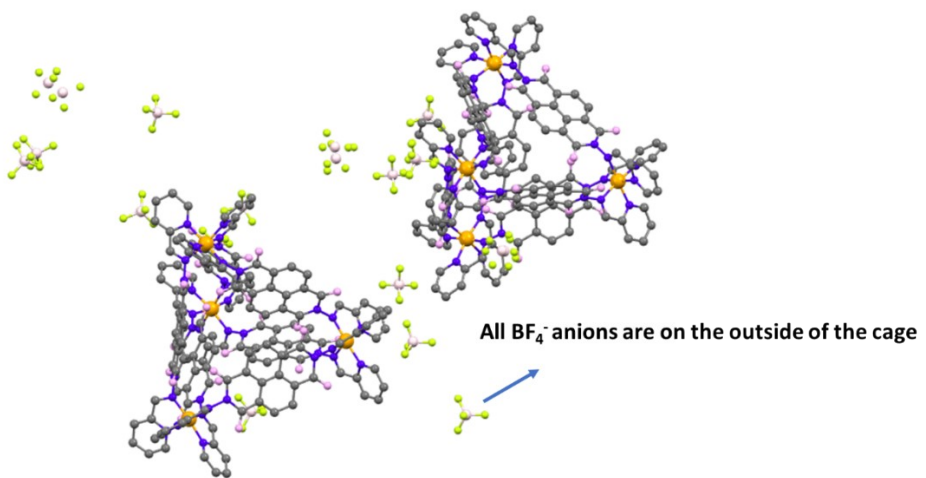
Fig. S16 Crystal structure of cage **2**. No anions were found inside the cage cavity.
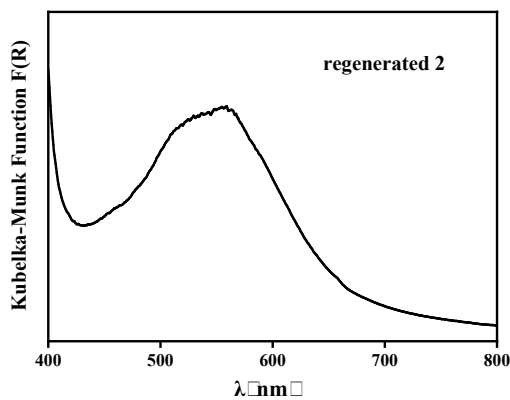
Fig. S17 Diffuse reflectance spectrum of regenerated **2**.
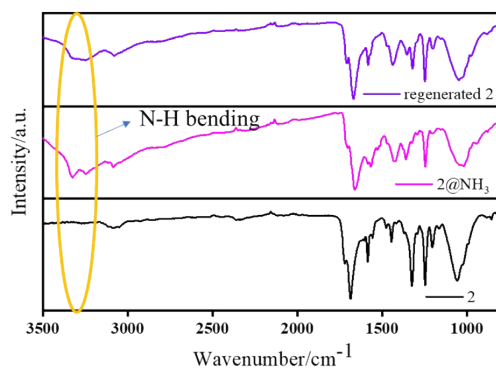
Fig. S18 FT-IR spectral of **2**@NH$_3$ and regenerated **2**. The absorption bands located at 3000-3500 cm^{-1} in **2**@NH3 and regenerated **2** are characteristic of N-H bending,[2] indicating that **2** adsorbs ammonia molecules, while the structure is irreversible after regeneration, in agreement with the results observed by PXRD, diffuse reflectance spectra and ^{57}Fe Mössbauer spectra.

Subcomponent ligand in reported cage

Subcomponent ligand in complex **1**

Subcomponent ligand in cage **2**
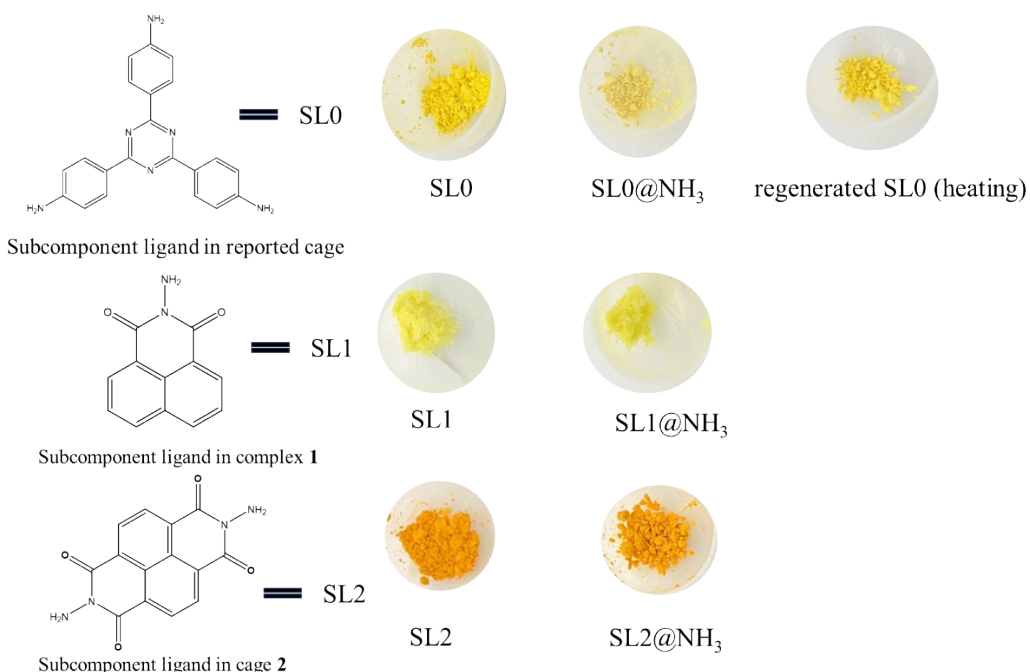
Fig. S19 The subcomponent ligand structures of the reported cage (SL0), **1** (SL1) and **2** (SL2) and the corresponding colour changes after exposure to ammonia vapor.

Table S3. Response time database of **1** for ammonia.

Time (min)	Times	R	G	B	H	S	B1
0	1	107	63	58	6	45	41
	2	112	62	57	5	49	43
	3	108	63	58	5	46	42
1	1	90	52	48	5	46	35
	2	89	50	47	4	47	34
	3	91	52	49	4	46	35
3	1	100	71	68	5	31	39
	2	101	72	68	7	32	39
	3	96	69	65	7	32	37
5	1	82	60	60	0	26	32
	2	76	55	55	0	27	29
	3	85	64	64	0	24	33
8	1	55	54	63	246	14	24
	2	52	52	60	240	13	23
	3	57	56	65	246	13	25
10	1	51	49	61	250	19	23
	2	50	48	60	250	19	23
	3	58	55	67	254	17	26
12	1	53	52	61	246	14	23
	2	52	52	60	240	13	23
	3	51	50	59	246	15	23
15	1	43	41	51	252	19	20
	2	48	46	57	250	19	22
	3	45	44	53	246	16	20

Table S4. Colour vectors for the response of **1** to different analytes.

Analytes	Times	R	G	B	H	S	B1
ammonia	1	107	63	58	6	45	41
	2	112	62	57	5	49	43
	3	108	63	58	5	46	42
ethanol	1	95	53	51	2	46	37
	2	97	53	51	2	47	38
	3	100	57	54	3	46	39
hydrazine hydrate	1	103	56	48	8	53	40
	2	98	51	44	7	55	38
	3	96	48	40	8	58	37
methanol	1	97	55	52	3	46	38
	2	94	52	49	3	47	36
	3	92	51	49	2	46	36
1,2-diaminocyclohexane	1	116	72	70	2	39	45
	2	115	70	70	0	39	45
	3	112	68	67	1	40	43
diethyl ether	1	115	69	65	4	43	45
	2	118	72	68	4	42	46
	3	119	71	66	5	44	46
isopropyl ether	1	109	63	60	3	44	42
	2	115	66	62	4	46	45
	3	110	64	60	4	45	43
THF	1	109	66	63	3	42	42
	2	103	60	57	3	44	40
	3	101	59	57	2	43	39
ethanolamine	1	109	60	50	10	54	42
	2	93	49	40	10	56	36
	3	93	50	38	13	59	36

ethyl acetate	1	122	70	66	4	45	47
	2	123	71	67	4	45	48
	3	119	64	63	1	47	46
dichloromethane	1	109	64	62	2	43	42
	2	104	59	58	1	44	40
	3	106	61	60	1	43	41
acetone	1	111	64	61	3	45	43
	2	120	72	69	3	42	47
	3	108	60	57	3	47	42
furfurylamine	1	98	65	64	1	34	38
	2	100	66	66	0	33	39
	3	103	69	69	0	33	40
water	1	105	61	58	3	44	41
	2	112	67	64	3	42	43
	3	93	54	51	4	45	36
aniline	1	95	66	66	0	35	37
	2	93	65	64	0	33	36
	3	96	66	69	1	36	37

Table S5. ^{57}Fe Mössbauer parameters of **1**, **1**@NH$_3$ and the regenerated **1**.

Sample	Spin State	A/A$_{tot}$ (%)	Mössbauer parameters		
			δ (mm s^{-1})	ΔE_Q (mm s^{-1})	$\Gamma/2$
1	Fe(II) HS (red)	100	1.00 (1)	2.56(2)	0.14(1)
1@NH$_3$	Fe(II) LS (blue)	33	0.32(3)	0.94(1)	0.20(3)
	Fe(II) HS (red)	41	1.00 (1)	2.61(2)	0.12(1)
	Fe(III) HS (yellow)	26	0.28(3)	0.42(1)	0.17 (1)
regenerated **1**	Fe(II) LS (blue)	24	0.33(3)	0.96(1)	0.16(1)
	Fe(II) HS (red)	45	1.00(1)	2.63(2)	0.13(2)
	Fe(III) HS (yellow)	31	0.29(3)	0.47(1)	0.18(1)

Table S6. ^{57}Fe Mössbauer parameters of **2** recorded at 80 K and 7 K**.**

Sample	Spin State	A/A$_{tot}$ (%)	Mössbauer parameters		
			δ (mm s^{-1})	ΔE_Q (mm s^{-1})	$\Gamma/2$
80 K	Fe(II) LS (blue)	46	0.45	0.36	0.29
	Fe(II) HS (cyan)	54	1.16	3.13	0.51
7 K	Fe(II) LS (blue)	44	0.45	0.37	0.30
	Fe(II) HS (cyan)	56	1.17	3.13	0.51

Table S7. Colour vectors for the response of **2** to other analytes.

Analytes	Times	R	G	B	H	S	B1
ammonia	1	56	56	61	240	8	23
	2	54	53	59	250	10	23
	3	55	55	61	240	9	23
ethanol	1	90	47	70	327	47	35
	2	91	47	71	328	46	35
	3	93	50	73	327	46	36
hydrazine hydrate	1	84	47	64	332	44	32
	2	93	53	71	332	43	36
	3	85	47	67	328	44	33
methanol	1	100	56	77	331	44	39
	2	105	59	82	329	43	41
	3	94	55	73	332	41	36

1,2-diaminocyclohexane	1	102	60	80	324	41	40
	2	97	59	79	322	39	38
	3	95	58	82	321	38	37
diethyl ether	1	92	50	69	332	45	36
	2	99	55	76	331	44	38
	3	100	53	77	329	47	39
isopropyl ether	1	93	49	70	331	47	36
	2	89	46	67	330	48	34
	3	94	52	71	332	44	36
THF	1	93	53	73	329	43	36
	2	93	51	72	329	45	36
	3	86	47	66	330	45	33
ethanolamine	1	99	54	77	329	45	38
	2	105	59	82	329	43	41
	3	106	59	82	330	44	41
ethyl acetate	1	92	52	78	330	43	36
	2	100	55	81	325	45	39
	3	94	52	79	331	44	36
dichloromethane	1	93	52	75	326	44	36
	2	97	54	79	325	44	38
	3	98	56	70	339	42	38
acetone	1	98	56	78	328	42	38
	2	96	52	75	328	45	37
	3	103	61	81	331	40	40
furfurylamine	1	94	57	79	324	39	36
	2	96	59	78	325	40	41
	3	90	56	77	322	37	35
water	1	98	51	73	331	47	38
	2	94	49	70	331	47	36
	3	97	52	73	331	46	38
aniline	1	93	53	66	340	43	36
	2	97	56	69	340	42	38
	3	91	50	64	339	45	35

Table S8. Response time database of **2** for ammonia.

2@NH₃							
Time (s)	Times	R	G	B	H	S	B1
0	1	96	52	72	332	45	37
	2	94	50	71	331	46	36
	3	100	55	76	331	45	39
60	1	70	48	67	308	31	27
	2	72	51	69	308	29	28
	3	73	52	70	308	28	28
90	1	53	49	56	274	12	21
	2	50	46	54	270	14	21
	3	53	49	56	274	12	21
180	1	56	56	61	240	8	23
	2	54	53	59	250	10	23
	3	55	55	61	240	9	23
300	1	55	53	60	257	11	23
	2	56	55	62	248	11	24
	3	52	52	58	250	10	22
360	1	47	46	52	250	11	20
	2	56	55	61	250	9	23
	3	55	54	61	248	11	23
480	1	49	47	59	250	20	23
	2	51	48	60	255	19	23
	3	50	47	59	255	20	23

Table **S9.** [57]Fe Mössbauer parameters of **2**, **2**@NH$_3$ and the regenerated **2.**

Sample	Spin State	A/A$_{tot}$ (%)	Mössbauer parameters		
			δ (mm s^{-1})	ΔE_Q (mm s^{-1})	$\Gamma/2$
2	Fe(II) HS-1 (red)	24	0.95	2.00	0.75
	Fe(II) HS-2 (violet)	17	1.07	2.74	0.41
	Fe(II) LS (blue)	59	0.37	0.30	0.34
2@NH$_3$	Fe(II) LS (blue)	21	0.38(2)	0.27(3)	0.12(4)
	Fe(II) LS-1 (cyan)	79	0.32(2)	0.62(1)	0.32(1)
regenerated **2**	Fe(II) LS (blue)	25	0.35(1)	0.27(3)	0.12(4)
	Fe(II) LS-1 (cyan)	75	0.32(2)	0.65(1)	0.28(3)

References

1. Y. Cui, J. Du, Y. Liu, Y. Yu, S. Wang, H. Pang, Z. Liang and J. Yu, *Polym. Chem.*, 2018, **9**, 2643-2649.

2. X. Chen, Y. Yu, C. Yang, J. Yin, X. Song, J. Li and H. Fei, *ACS Appl. Mater. Interfaces*, 2021, **13**, 52765–52774.